

Multi-Transient Electromagnetics (MTEM) – controlled source equipment for subsurface resistivity investigation

Bruce Hobbs, MTEM Ltd, Edinburgh, UK
 Anton Ziolkowski, MTEM Ltd, Edinburgh, UK
 David Wright, MTEM Ltd, Edinburgh, UK

SUMMARY

The technique of Multi-Transient Electromagnetic (MTEM) surveying is described and the measurements required to achieve good resolution are detailed. Field experience with a number of surveys has led to rapid development of instrumentation and methodology. The large gain in signal-to-noise ratio through the use of Pseudo-Random Binary Sequences (PRBSs) as input is demonstrated.

Keywords: time domain, galvanic source, instrumentation, Pseudo-Random Binary Sequences

INTRODUCTION

The MTEM method uses a current bi-pole source and a line of bi-pole receivers (Wright et al., 2002; Ziolkowski et al., 2005; Wright et al., 2005). Electric current is injected at the source and measured; the voltage between each pair of receiver electrodes is also measured. By deconvolving the measured output voltage for the measured input current the impulse response of the earth is recovered. This may be integrated to recover the step response, which is the normal input to the inversion process to recover subsurface resistivities. The form of the transient electric current input may be a simple step change, caused by a sudden reversal in current for example, or a pseudo-random binary sequence (PRBS) of such changes, or any other transient form. MTEM Ltd's current system has 40 receiver channels and the physical set-up is similar to that of seismics, with a source (or "shot") and a receiver spread – the source and receiver spread may then be "pushed" along a profile of interest. The technique, with a simple step function source, is illustrated in Figure 1.

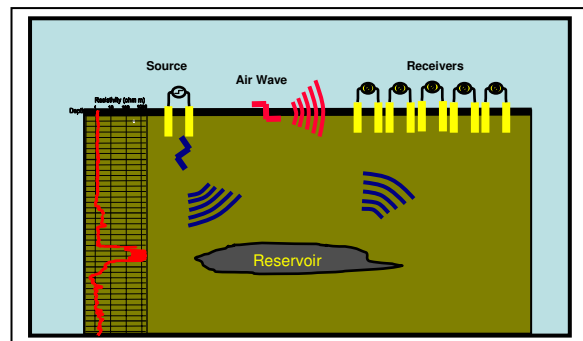


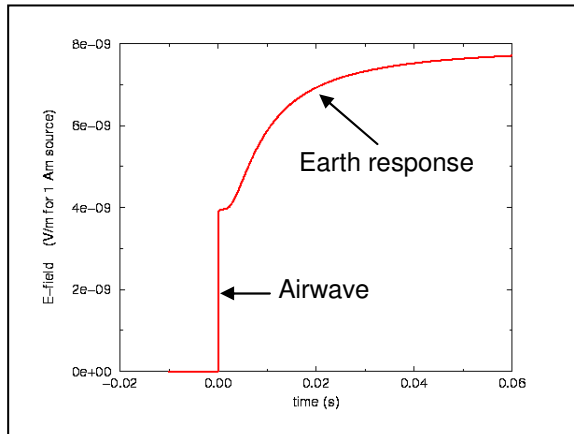
Figure 1. Source and receivers at the surface of the earth. A typical resistivity well log is shown on the left and the technique aims at detection and delineation of the reservoir.

The step change generated at the source travels along the surface of the earth at close to the speed of light – this is termed the airwave. The change also travels through the earth, sampling regions of differing resistivity. The airwave passes all receivers before the signal from the subsurface arrives. The form of the signal from the subsurface is dependent on the subsurface resistivity distribution.

EARTH RESPONSE FUNCTIONS

To illustrate the method, suppose the subsurface consists of a uniform halfspace of resistivity $20 \Omega\text{m}$ and the source is a bipole of moment 1 Am (i.e a current of 1 Amp and a source electrode separation of 1 m). Then the measurement at the receiver would be as shown in Figure 2(a).

a



b

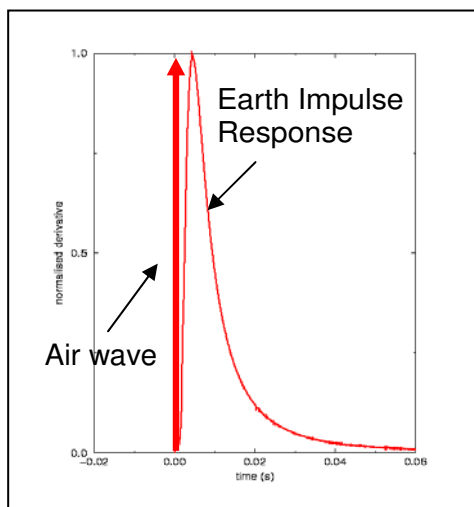


Figure 2. (a) The step response and (b) the impulse response at an offset of 1000 m for a 1 Am source over a uniform halfspace of resistivity $20 \Omega\text{m}$.

The step response (the electric field) at a receiver on land starts with an instantaneous increase at time $t = 0$ (representing the airwave), followed by a period of little change after which the transient responds to the subsurface resistivity. The response varies with offset. Since the derivative of a step is a delta function, or impulse, the derivative of the step response is the

earth's impulse response. This is shown in Figure 2(b). The impulse response consists of a delta function at time $t=0$ (representing the airwave) followed by the earth's impulse response arising from the subsurface distribution of resistivity. In practice the recording system will be band limited and the airwave will appear as a sharp high amplitude peak relative to the earth's impulse response.

When a resistive layer is added to the halfspace, the earth's response increases in amplitude and the peak of the impulse response arrives earlier, since the disturbance travels faster through high resistivity material.

EVOLUTION OF MTEM EQUIPMENT

1. Prototype equipment

Demonstration equipment was designed and built in The University of Edinburgh, in Scottish Enterprise Proof of Concept Project 4-ENO 004, to meet the specifications required by the MTEM method (Wright et al., 2002; Ziolkowski et al., 2003). Eleven two-channel recording units were made, ten for the receiving array and one to record the system response. Each unit had its own GPS receiver and on-board CPUs for analogue-to-digital conversion, data recording and storage, and communication via fast transmission cable to a central recording PC. Where communications were difficult across dense woods, independent GPS-synchronised recording PCs were used. A newly designed on-line QC system enabled the layout and status of the system to be checked and the incoming data on all channels to be viewed simultaneously, before and after stack. The current source was a Zonge transmitter CGT-30, powered by a ZMG-30 generator, that switched DC current between opposite polarities.

Data acquisition using this equipment took place over 9 days in December 2004. A total of 40 source positions were fired with the response recorded simultaneously on 20 channels. Offsets ranged from 300 m to 4600 m ; for the largest offsets the source length was increased from 100 m to 300 m or 500 m in order to increase the signal strength. Over a million individual traces were collected. The acquisition parameters are detailed in Table 1.

Data quality was generally excellent with a signal-to-noise ratio (SNR) of 60 dB being typical at 1500 m offset and with SNR higher at shorter offsets. In areas where the SNR is below 35 dB this is due to high amplitude cultural noise near the receiver. Figure 3 shows the SNR of all the data.

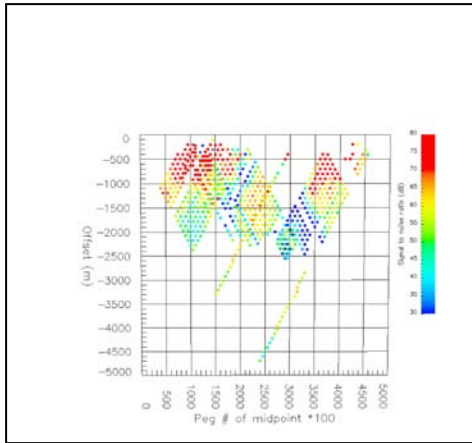


Figure 3. Signal to noise ratio of the MTEM data.

Figure 3 also shows the subsurface coverage achieved – the target depth was around 500m for which offsets in the range 1000m – 2250m are most appropriate.

2. Second generation equipment (Helium)

Following establishment of the MTEM company in 2004, 40 new ruggedised receiver units were built, with extended acquisition capabilities. During fieldwork, 20 of these two-channel receivers are generally active, giving a 40 channel system. Other receiver units are laid ahead of the line enabling the spread to be “pushed” along the profile efficiently. Much effort has been devoted to improving the signal-to-noise ratio and as a consequence the source is now driven by a Pseudo-Random Binary Sequence (PRBS). Table 2 details the acquisition parameters for this second system.

The second generation system was employed in sub-zero conditions in northern Alberta and in the extreme heat of India. A major development for this second system was the employment of PRBSs in place of simple step changes in the current at the source. Stacking N records from step changes gives a SNR gain of \sqrt{N} . The theoretical gain, G , in SNR using a PRBS of order p (and thus length $M=2^p-1$) is $\sqrt{M} < G < M$. The memory capacity of the second generation equipment led to the limit $p=12$, giving a

theoretical SNR increase of between 36dB and 72dB. We cannot afford not to take advantage of this enormous potential gain and so memory capacity has been increased in the next generation of equipment to allow use of longer PRBSs. The sampling rate is also a factor: oversampling reduces the processing gain.

3. Third generation equipment (Jura)

Third generation equipment is currently under test and field surveys will commence in August 2006. Sampling and source frequencies are now independent and their range has been extended to cope with a larger range of target depths and background resistivities. A substantial increase in memory capability enables the use of much longer PRBSs resulting in improved signal-to-noise ratios. Table 3 shows the new acquisition parameters.

CONCLUSIONS

Experience gained in field acquisition in Europe, Canada and India has led to a design specification for third generation MTEM recording equipment which is shortly to be field tested. The use of PRBSs and a rigorous approach to parameter specifications has led to increasing improvements in signal-to-noise ratios and hence target detectability.

REFERENCES

- Ziolkowski, A., Hobbs, B., Wright, D., Dawes, G. and Russel, S., 2005. Transient EM detects sub-surface gas. Extended Abstract H047, 67th EAGE Conference, Madrid.
- Wright, D., Hobbs, B. and Ziolkowski, A. 2005. MTEM Demonstration survey in France. Expanded Abstract EM 3.6, 75th SEG Annual Meeting, Houston.
- Wright, D., Ziolkowski, A., and Hobbs, B., 2002. Hydrocarbon detection and monitoring with a multichannel transient electromagnetic (MTEM) survey. *The Leading Edge*, 21, 852-864.

Table1: Acquisition parameters for the demonstration survey.

Amplitude of current switch	20-50A
Voltage across source electrodes	750-1000V
Sampling frequency	15kHz
No. of records per source position	Unlimited, but typically 1500-2500
Source electrode separation	100m - 500m
Receiver electrode separation	100m

Table 2: Acquisition parameters for the second generation equipment.

Length of PRBS	1 - 4095 ($2^{12} - 1$)
Amplitude of current switch	20-50A
Voltage across source electrodes	750-1000V
Sampling frequency	600Hz - 15kHz
No. of records per source position	Unlimited, but typically 20 - 1000
Source electrode separation	50m - 500m
Receiver electrode separation	50m - 100m

Table 3: Acquisition parameters for the third generation equipment.

Length of PRBS	1 - 262,143 ($2^{18}-1$)
Amplitude of current switch	20-80A
Voltage across source electrodes	750-1000V
Sampling frequency	200Hz - 32kHz
No. of records per source position	Unlimited, but typically 1 - 10
Source electrode separation	50m - 500m
Receiver electrode separation	50m - 200m

Some parameter sensitivity tests to TEM method

Xingong Tang, Peking University, Department of Geophysics, Beijing, P.R. China
 Wenbao Hu and Liangjun Yan, Yangtze University, Key Laboratory of Exploration Technologies for Oil and Gas Resources of MOE, Jingzhou Hubei, P.R. China

SUMMARY

A series of models are designed to test the influences of some parameters such as transmitter-receiver layouts, resistivity of surface layer, surrounding medium and basement to a given 3D conductive anomaly in the layered earth model by transient electromagnetic (TEM) method. The forward modeling procedure used is formulated with volume integral equation based on tensor Green's function. The response of electromagnetic components are first calculated in frequency domain and then transformed to time domain by digital filtering. Through a series of modeling, it shows that S-s layout is more suitable for surveying shallow target than AB-s array. The transient responses of e_x component is larger if the surface layer is resistive. While V_z component is not sensitive to the resistivity of the surface layer. The more conductive the surrounding layer where the anomaly exist, the larger the transient responses, no matter high or low the surface layer resistivity is. The models also illustrate that S-s layouts are not sensitive to the variation of basement resistivity..

Keywords: TEM, sensitivity, 3D forward modeling

INTRODUCTION

Controlled source electromagnetic methods (CSEM) are now widely used for resource and engineering exploration. The time domain methods are preferred for structure mapping since the vertical resolution is believed higher than frequency domain methods. Different configuration of setup for field survey can be used to probe different type of targets at various depth, and the source current can be delivered by loop or grounded wire. When the steady source current in the circuit is suddenly switched off, a secondary currents will be induced in the conductive stratum in accordance with the Maxwell's EM induction law. The induced secondary field decays with time as the current gradually dissipate on account of the electrical resistance in the conductor. One of the advantages of the TEM method is that it only measures the secondary or scattering field after the primary current is turned off so it is not influenced by the primary field (Strack, 1992). The field responses of different components may have different behaviour to different model parameters (Tang et al.,2005). This work is to check the sensitivity of AB-s and S-s setups to the conductive anomalous body, body depth, surface layer, bed

Table 1 The parameters of the 4-layered earth model.

Depth m	Resistivity $\Omega.m$	Alternative value
50	50(surface)	10/2000
300	500(surrounding)	5000/2000/100
1000	10	
∞	500	50/5000

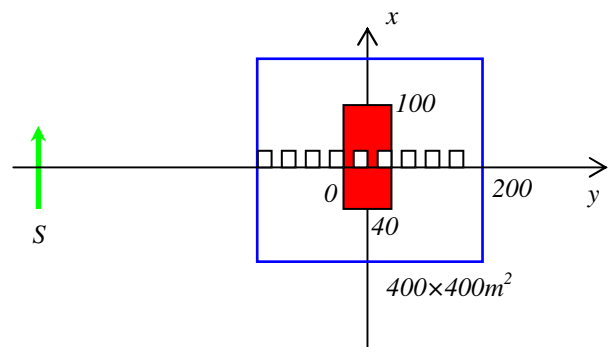


Figure 1. Diagram showing the transmitter and receivers layouts. The green arrow is the dipole source in AB-s array. The blue square is the loop source and the mini square inside means receivers. The red one is the 3D conductive anomaly.

formation and basement resistivity by numerical modeling.

MODEL DESIGN

Assume a three dimensional anomalous body with conductivity $\sigma=0.1\text{S/m}$ and the size of $200\times 80\times 30\text{ m}$ is sit in a four layer earth model, the parameters of the earth model are listed in Table 1. A series of numerical modeling is carried out to find in which cases the transient electromagnetic method (TEM) is most sensitive for detecting the target. Although some results are familiar to us, it is still interesting to prove the validity of the knowledge we have learned from books and papers before by numerical modeling.

Four kind of testing setups are designed for this checking. First, sensitivity checking for different layouts of the transmitter and receivers such as AB-s and S-s to test which setting is more suitable to detect shallow target. The model setup shown in Figure 1 is used for calculation and discussion. Secondly, sensitivity checking for changing the resistivity of the surface layer. Thirdly, for changing the resistivity of the surrounding layer where the 3D anomaly exists. In our models it is the second layer. Finally, for changing the resistivity of the basement layer.

In the whole process of modeling, the size and resistivity of the 3D body, the transmitter and receivers keep unchanged in order to compare the results quantitatively.

For long offset transient electromagnetic (LOTEM) method, the ground source is usually an grounded horizontal electrical wire of finite length which can be considered as a dipole source if the distance of transmitter and receivers is large enough. This is the so-called AB-s setup. The center of dipole source is located at $y=-6000\text{m}$ and offsets used in AB-s modeling is 5800 m to 6200 m with the interval of 10 m and the current moment is 200 Am-m .

For central loop (S-s) layout, the transmitter can be a square or a rectangular loop. For modeling convenience, a square loop with dimension of $400\times 400\text{ m}$ is used. According to the different layouts, vertical or horizontal component of the secondary electric and magnetic field, the time derivative of vertical magnetic component V_z and/or electric field component e_x are measured.

The anomalous body is divided into 240 cells in numerical computation and only one quarter is involved in calculation for speeding the computation according to the group theory (Newmn et al., 1986).

RESULTS AND ANALYSIS

From figure 2, we can see that AB-s can comparatively more easily detect the conductive target buried both in deep and shallow depth. S-s coupling, on the other hand, is difficult to detect the deep anomaly but it can survey the shallow target more clearly, which we can quantitatively see from Table 2. So the following models will focus on S-s layouts due to the shallow target.

From Table 2, it shows that the detectability of TEM to the conductive anomaly will change as changing the resistivity of the surface layer. Generally speaking, the higher the resistivity of the surface layer, the easier to be detected by S-s TEM method, especially for e_x component, and vice versa. It is because that conductive surface attracts more current due to the current channeling effect, so less current can reach deeper depth. While V_z component is nearly not affected by the resistivity of the surface layer, which can be seen from model 5, 7 and 8. In other word, V_z component is less sensitive to the resistivity of the shallow surface layer.

For S-s coupling, when the resistivity of the surface layer fixed, it shows that more conductive the surrounding layer where the anomaly exist, the larger the transient responses, no matter high or low the surface layer resistivity is, which can be seen from results of model 9,10 as well as 7,12 and 13.

There are no changes to the transient responses when the resistivity of basement is altered. This is maybe because the basement (nearly 2000 m) is too deep for S-s setting to give enough responses and illustrates it is not sensitive to the variation of the resistivity of basement in S-s survey for the designed layout.

The transmitter-receiver combination and model parameters as well as their results are listed in table 2 in detail. "Y" means the target can be detected and "N" means can't. Only the transient responses of models 1, 5 and 8 are shown in Figure 2.

CONCLUSION

Transient EM method can be used to explore subsurface anomalies. For AB-s setting, which is often used as LOTEM in field survey, it is easily to detect the conductive anomalies both in deep and shallow depth. For S-s layouts, it is difficult to detect the deep depth, but it is more suitable for shallow targets exploration.

REFERENCES

Strack, K.M.. Exploration with Deep Transient

Electromagnetic Method. *Elsevier*. 1992.

1986, **51**: 1608-1627.

Nabighian, M.N. *Electromagnetic Methods in Applied Geophysics*. SEG. 1987.

Tang Xingong, Hu Wenbao, Yan Liangjun. The Detectability of Transient electromagnetic method to multiple three-dimensional bodies with valley topography, *Seismology and Geology* (in Chinese), 2005, 27(2),316-323.

Newmn, G.A., Hohmann, G.W., and Anderson, W.L., Transient electromagnetic response of a three-dimensional body in a layered earth, *Geophysics*,

Table 2 The transmitter-receiver combination, model parameters and modeling results

Model	Layouts and Body depth	Component	Range of secondary field	Detectability
model 1	AB-s Body in 100m	e_x	$-7.12e^{-12} \sim 1.30e^{-12}$	Y
		V_z	$-1.02e^{-18} \sim 1.11e^{-18}$	Y
model 2	AB-s Body in 2000m	e_x	$-1.55e^{-15} \sim 3.22e^{-16}$	Y
		V_z	$-1.26e^{-21} \sim 1.32e^{-21}$	Y
model 3	AB-s Body in 1000m	e_x	$-1.338e^{-15} \sim 6.43e^{-16}$	Y
		V_z	$-2.66e^{-20} \sim 2.77e^{-20}$	Y
model 4	S-s Body in 2000m	e_x	$-2.0e^{-18} \sim 2.0e^{-18}$	N
		V_z	$-2.9e^{-22} \sim 8.59e^{-22}$	N
model 5	S-s Body in 100m	e_x	$-1.39e^{-10} \sim 1.39e^{-10}$	Y
		V_z	$-1.03e^{-16} \sim 2.74e^{-16}$	Y
model 6	S-s Body in 1000m	e_x	$-1.21e^{-15} \sim 1.21e^{-15}$	N
		V_z	$-2.5e^{-20} \sim 6.64e^{-20}$	N
model 7	S-s, Body in 100m, surface is $10\Omega m$	e_x	$-3.07e^{-11} \sim 3.07e^{-11}$	Y
		V_z	$-1.03e^{-16} \sim 2.74e^{-16}$	Y
model 8	S-s, Body in 100m surface is $2000\Omega m$	e_x	$-1.02e^{-9} \sim 1.02e^{-9}$	Y
		V_z	$-1.03e^{-16} \sim 2.73e^{-16}$	Y
model 9	S-s, Body in 100m, surface is $500\Omega m$, surrounding is $100\Omega m$	e_x	$-9.72e^{-10} \sim 9.72e^{-10}$	Y
		V_z	$-1.94e^{-16} \sim 5.13e^{-16}$	Y
model 10	S-s Body in 100m, surface is $2000\Omega m$, surrounding is $5000\Omega m$	e_x	$-3.19e^{-10} \sim 3.19e^{-10}$	Y
		V_z	$-2.06e^{-17} \sim 5.45e^{-17}$	Y
model 11	S-s Body in 100m surface is $2000\Omega m$, surrounding is $2000\Omega m$	e_x	$-5.97e^{-10} \sim 5.97e^{-10}$	Y
		V_z	$-4.32e^{-17} \sim 1.143e^{-16}$	Y
model 12	S-s, Body in 100m surface is $10\Omega m$, surrounding is $5000\Omega m$	e_x	$-2.41e^{-12} \sim 2.41e^{-12}$	Y
		V_z	$-2.06e^{-17} \sim 5.45e^{-17}$	Y
model 13	S-s, Body in 100m, surface is $10\Omega m$, surrounding is $2000\Omega m$	e_x	$-6.78e^{-12} \sim 6.78e^{-12}$	Y
		V_z	$-4.32e^{-17} \sim 1.144e^{-16}$	Y
model 14	S-s, Body in 100m, surface is $2000\Omega m$ basement is $5000\Omega m$	e_x	$-1.02e^{-9} \sim 1.02e^{-9}$	Y
		V_z	$-1.03e^{-16} \sim 2.73e^{-16}$	Y
model 15	S-s, Body in 100m, surface is $2000\Omega m$ basement is $50\Omega m$	e_x	$-1.02e^{-9} \sim 1.02e^{-9}$	Y
		V_z	$-1.03e^{-16} \sim 2.73e^{-16}$	Y

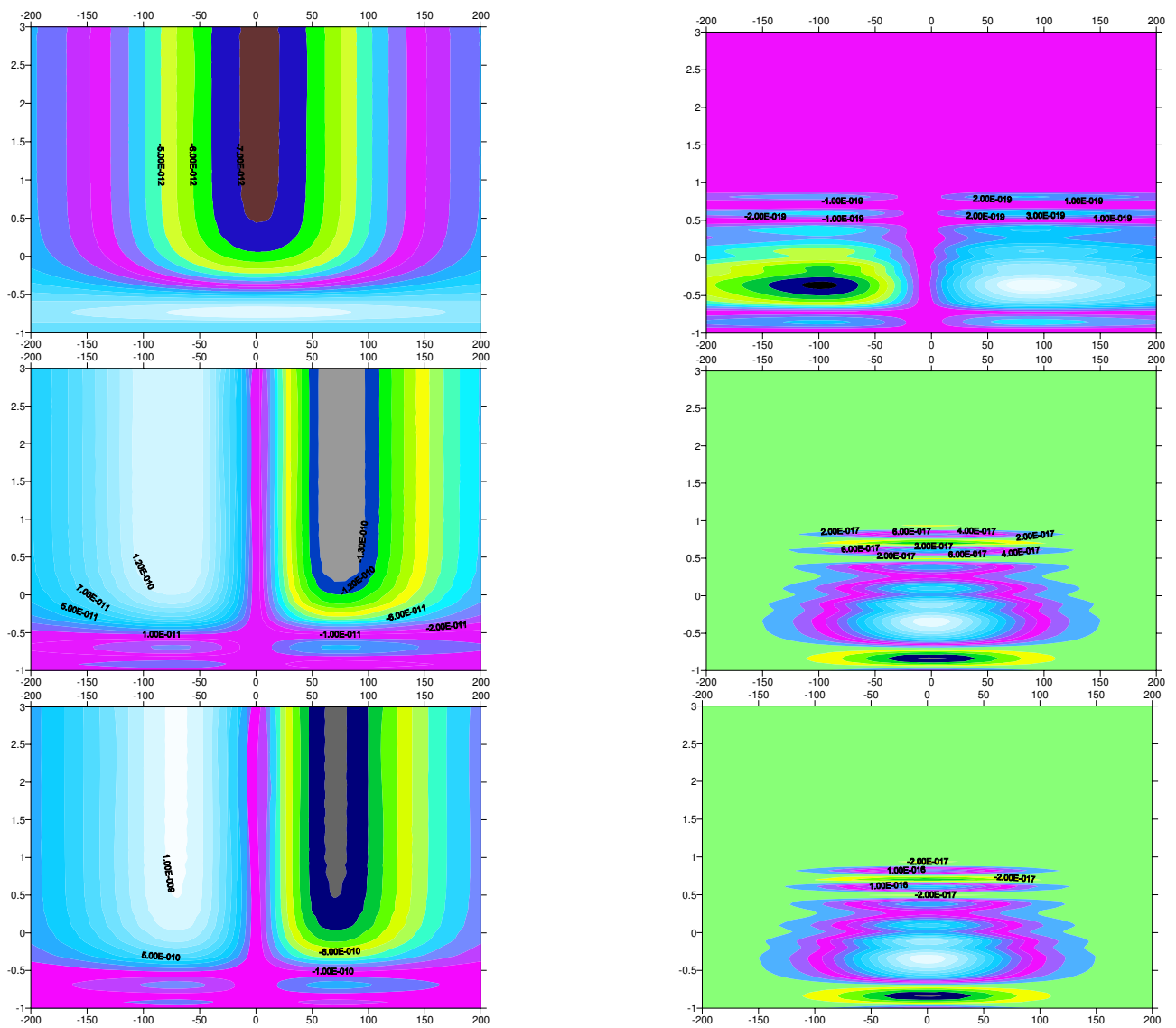


Figure.2. The secondary fields of model 1, 5 and 8. The left is e_x component and the right V_z component.

Research on the Influence of Abnormal Body Between the Source and Exploration Area on the Target Body

Ruo Wang, Miao-yue Wang, Qing-yun Di, Institute of Geology and Geophysics, Chinese Academy of Sciences, Beijing, China

SUMMARY

In the field work of control-source magnetotelluric method, the separate between the transmitter and the receiver is more than 3~5 times skin depth, so it is important to study the influence of the abnormal body in this area on the target body in the exploration area .

In this paper, it is discussed that the influence of the abnormal body out of exploration area with different resistivity, size and location on the target body due to a line source in 2D. When the abnormal body out of the exploration area is a conductor, the lower the resistivity, the larger the influence on the exploration area is; the larger its size, the heavier the influence is; the shallower its buried depth, the larger the influence range is; the deeper its buried depth, the smaller the influence on the body in the shallow exploration area is. When the abnormal body is resistive, the similar influence rules can be obtained, but the influence is very small.

In order to know how about the inversion result only using the exploration area data, we compare the inversion results by using the whole research area (including area from source position to the exploration area right border) data to that by using the data in the exploration area only. It is proved that the horizontal position of the target body can be inverted accurately except for the depth deeper than the predicted one when executing inversion with the exploration area data only.

Keywords: line source; the abnormal body between the active source and the exploration area; influence.

INTRODUCTION

For magnetotelluric method with active source, the source's influence is obvious; Kuznetsov(1982) and Zonge and Hughes(1988) obtained the conclusions that the active source has overprint influence on the exploration area. Boschetto(1991) discussed the influence of the abnormal body lying below the active source on the homogeneous half space with integral equation method. As we know, the transmitter-receiver separation is 3~5 times skin depth for the control source magnetotelluric in frequency domain. It is necessary to know the influence of the abnormal body between the source and exploration area on the target body.

In practice, the abnormal bodies between the source and the exploration area don't be taken into consideration till now when an inversion scheme is executed. It is need know how about the influence of

the abnormal bodies outside the exploration area on the inversion result.

Here, the influence of the abnormal body locating between the source and exploration area on the target body is discussed by using finite element method in two-dimension due to a line source, then the inversion results with the whole research area data and the exploration area are compared, which are obtained using the inversion scheme developed by Xinyou Lu (1999).

DESIGNING OF MODEL

Figure 1 shows the model used in the study work. There is a target conductor with size 300m×300m in the explored area, which is called the first conductor in the following discussion, whose resistivity is $10\ \Omega\text{m}$, and the background resistivity is $100\ \Omega\text{m}$. The centre of this abnormal body is located at 300m in depth; the

distance from this centre to source is 3000m, which mean that the first conductor's centre is located at node 64 in horizontal and node 43 in vertical. There is another abnormality (we call it as second conductor or resistive body according to its resistivity) locating between the source and the exploration area, whose size is variable from small to large, which is 300m×300m 1000m×500m 1000m×2000m separately. We will discuss the different influence of the second abnormal body on the first conductor in exploration area when its size, resistivity or location changes.

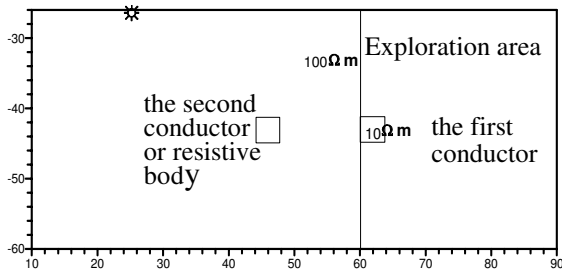


Fig.1 the model sketch map

Figure 2 shows the apparent resistivity sections after forward modeling with the model mentioned above when the second conductor or resistive body is not exist. The abnormal is clearly though the resistivity difference between the abnormal and the wall rock is small.

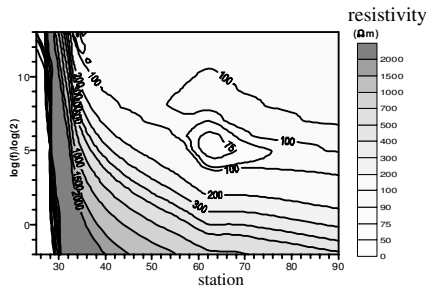


Fig.2 the forward modeling result of low resistivity prism when the second conductor or resistive body is not exist

THE INFLUENCE OF THE ANOMAL BODY ON THE EXPLORATION AREA

When the second conductor is buried at 300m in depth, the apparent resistivity curve above the first conductor's centre is shown in figure 3.

Figure 3(a) displays the apparent resistivity response above the first conductor's centre when the second conductor is located at 1500m away from the source. In figure 3(a), there are seven curves; each illustrates the apparent resistivity responds above the first conductor when the second conductor has different resistivity and size. The curves have three colors: red, black and blue,

which represent three cases, the red curve expresses the original curve when the second conductor does not

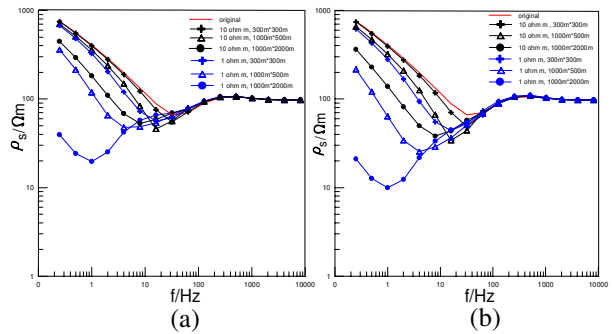


Fig.3 the apparent resistivity responses above the first conductor locating in the exploration area when the second conductor with different size is located at 300m in depth (a) the second conductor is located at 1500m away from the source (b) the second conductor is located at 2000m away from the source

exist, the blue and black curve express the second conductor's resistivity is 10 Ω m and 1 Ω m , respectively. There are three symbols on the curves, which mean different size of the second conductor. '+' means that the size is 300m×300m, 'Δ' means 1000m×500m and '·' means 1000m×2000m.

Figure 3 (a) shows the apparent resistivity curve depart from the original one when the survey frequency is lower than 128Hz. The offsets of the blue curves to the red curve are more than that of the black curves to it, which means that the lower the resistivity of the second conductor, the larger its influence on the exploration area is. The curves with same color show that the second conductor's influence on the exploration area is proportional to its size, the bigger the size, the larger the influence is.

Figure 3 (b) shows the apparent resistivity curves above the first conductor's centre in the exploration area when the second conductor locate at 2000m far from the active source and indicates the same rules as figure 3 (a).

Comparing figure 3 (b) to 3 (a), we found that the apparent resistivity value with same color and same symbols at frequency lower 100Hz in figure 3 (b) is lower than that in 3 (a), which mean the second conductor affect the exploration area more when its location is far from the active source or more close to the exploration area.

In order to display the second conductor's influence on the response of the first conductor visual able, figure 4 shows the pseudo-section corresponding to the cases in figure 3. The active source is located at the left-upper corner.

Figure 4(a1) ~ (a3) (b1) ~ (b3) show the cases when the second conductor's resistivity is $10 \Omega m$, the former is corresponding to the case when the second conductor is located at 1500m away from the source, and the latter is corresponding to the case the conductor located at 2000m away from the source. From the six pseudo-sections, we found the response of the first conductor is small contrasting to the second conductor's response in figure 4(a1) ~ (a3), but large in figure 4(b1) ~ (b3), the anomaly of the first one is almost overlapped by the second conductor's response except for in figure 4(b1) where the second conductor's size is small.

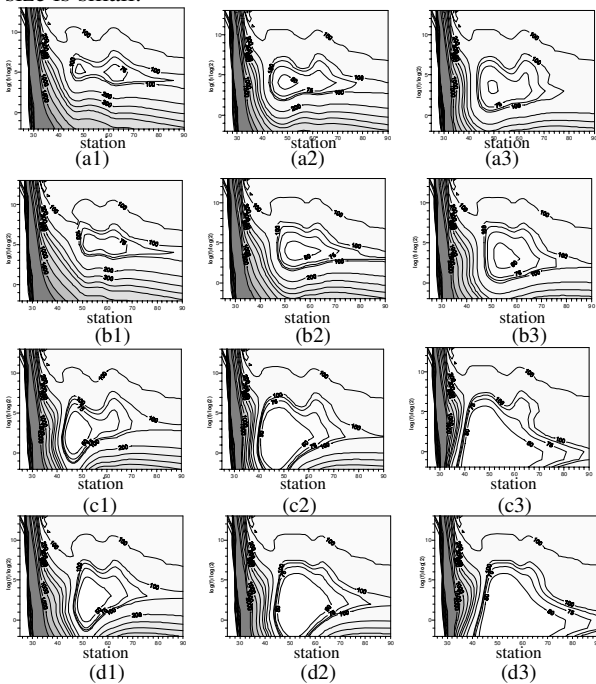


Fig.4 the apparent resistivity response sections when the second conductor with different resistivity and size locates at 300m in depth, the source is located at the up-left corner of each section. The vertical axis is representing the logarithm of survey frequency with base 2; the horizontal axis is representing the survey points or the mesh node in horizontal. The second conductor's resistivity, size and the position away from the source respectively is:

- (a1) $10 \Omega m$, $300m \times 300 m$, 1500 m (a2) $10 \Omega m$, $1000 m \times 500 m$, 1500 m (a3) $10 \Omega m$, $1000 m \times 2000 m$, 1500 m
- (b1) $10 \Omega m$, $300 m \times 300 m$, 2000 m (b2) $10 \Omega m$, $1000 m \times 500 m$, 2000 m (b3) $10 \Omega m$, $1000 m \times 2000 m$, 2000 m
- (c1) $1 \Omega m$, $300 m \times 300 m$, 1500 m (c2) $1 \Omega m$, $1000 m \times 500 m$, 1500 m (c3) $1 \Omega m$, $1000 m \times 2000 m$, 1500 m
- (d1) $1 \Omega m$, $300 m \times 300 m$, 2000 m (d2) $1 \Omega m$, $1000 m \times 500 m$, 2000 m (d3) $1 \Omega m$, $1000 m \times 2000 m$, 2000 m

When the second conductor's resistivity is $1 \Omega m$, the pseudo-sections are shown in figure 4 (c1) ~ (c3) and figure 4 (d1) ~ (d3). The former represent the second conductor located at 1500m away from the source, the latter represent the second conductor located at 2000m. The six sections give the same conclusion as in the figure 4 (a1) ~ (b3). Comparing one case to another, we

found that the second conductor with lower resistivity affect the exploration area more than that with higher resistivity.

When the second conductor is buried 10m in depth, the curves above the first conductor center has the similar basic characters with that in figure 3, but the frequency of the apparent resistivity curve departing from the original one is higher than that in figure 3.

From the study above, we also know that the lower the second conductor's resistivity, the larger the influence on the exploration area is; the nearer the second conductor's position to the first conductor, the larger the influence on the exploration area is.

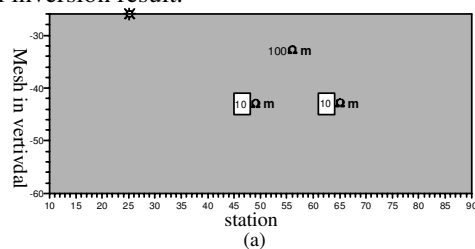
When the resistive body is located between the exploration area and the active source, what influence does it has on the exploration area? In order to discuss this problem, we set the resistivity of the resistive body $1000 \Omega m$ and $2000 \Omega m$ respectively, but keep the first conductor's resistivity as same as above examples. The research result shows that the resistive body has little influence on the exploration area.

INVERSION

Through the discussion above we know that the conductor located between the exploration area and the active source has strong influence on the exploration area, but the resistive body's influence is small. In practice, we don't know what medium exist between the source and the exploration area, so generally the medium between source and the exploration area are neglected in the inversion, whether the inversion result is reliable or not, we study it as follow.

The inversion method developed by Xinyou Lu (1999) is used here. We do the inversion to the cases that the second conductor is located at 300m in depth while the horizontal location away from the source is 1500m. The model is shown in figure 6 (a), where "⚙" represents the source position.

The data in the research area (including area from source position to the exploration area right border) and the data in the exploration area are inverted respectively, and the tenth iteration result act as the final inversion result.



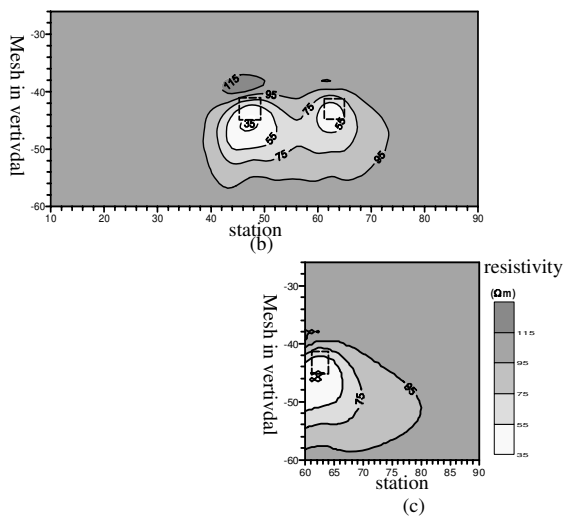


Figure 6 (b) show that the two abnormal bodies are both inverted exactly except for the depth of the target body is deeper than that of the model, but the horizontal position is correct. Figure 6 (c) show the inversion result using the exploration area data, the conductor is obtained, but the constructed conductor's volume is enlarged, and the depth is deeper a little than that shown in figure 6 (b).

CONCLUSIONS

When the abnormal body outside of the exploration area is a conductor, the influence is very strong. The lower the resistivity, the larger the influence on the exploration area is; the larger the size, the heavier the influence is, but when the resistivity is low ($1 \Omega m$), the influence is large even if the size is small. The influence on the exploration area from shallow to deep is large when the abnormal body out of the exploration area is buried shallow. However it buried deeper, the influence on the shallow of the exploration area is smaller than that on the deeper. The closer the abnormal body's position to the exploration area, the larger the influence is.

When the abnormal body outside of the exploration area is resistive, the influence feature is similar to the one caused by a conductive body. The closer to the exploration area it locating, the larger the influence is. The shallower it buried, the larger the influence on the shallow part of exploration area is. The bigger the size, the larger the influence is. But the influence is much less than that caused by a conductive body.

The inversion result using the whole research area data can obtain the abnormal body's position more precise. According to our research result, when the data is inverted by using the inversion method mentioned in

our paper, the conductor in exploration area can be inverted clearly. But the resolution is lower and the depth is deeper than the inversion result using the whole research area data, while the horizontal position is inverted accurately.

All of this research result will become significance guidance to recognize the field data and the inversion results by CSAMT method.

REFERENCES

- Bartel, L.C. and Jacobson, R.D.. Results of a controlled-source audio frequency magnetotelluric survey at the Puhimau thermal area, Kilauea Volcano, Hawaii, *Geophysics*, 1987(5), 665-677
- Boschetto N. B. and Hohmann G. W., Controlled-source audiofrequency magnetotelluric responses of three-dimensional bodies. *Geophysics*, 1991, 56(2): 255-264
- Kuznetsov, A. N., 1982, Distorting influences during electromagnetic sounding of horizontally non-uniform media using an artificial field source: *Izvestiya, Earth Physics*, 18, 130-137
- Routh, P.S. and Oldenburg, D.W.. Inversion of controlled-source audio-frequency magnetotelluric data for a horizontal-layered earth. *Geophysics*. 1999 (6), 1689-1697
- Xinyou Lu, Martyn Unsworth and John Booker. Rapid relaxation inversion of CSAMT data. *Geophys.J.Int.* 1999. 138, 381-392.
- Yamashita and Hollof. CSAMT case histories with a multi-channel CSAMT system and discussion of near-field data correction: phoenix Geophys., Ltd. 1985.
- Yutaka Sasaki, Yoshihiro Yoneda et al. Resistivity imaging of controlled-source audio frequency magnetotelluric data. *Geophysics*, 1992 (7): 952-955
- Wannamaker, P.. Tensor CSAMT survey over the Sulphur Springs thermal area, Valles Caldera, NewMexico, U.S.A., Part : Implications for structure of the western caldera, *Geophysics*, 1997(2): 451-465.
- Zonge, K.L. and Hughes, L.J. Controlled source audio-frequency magnetotellurics. in Nabighian M.N.,ED. *Electromagnetic methods in applied geophysics*, 2, Practice: Soc. Explor. Geophys., Tulsa. 1988.

Improving electromagnetic induction detector technology in humanitarian demining

R.C. Bailey, University of Toronto, Departments of Geology and Physics, Toronto, Canada
G.F. West, University of Toronto, Department of Physics, Toronto, Canada

SUMMARY

A variety of metal detectors using electromagnetic induction (EMI) are available for the detection of buried metallic targets in general and for humanitarian demining in particular. Detector designs suitable for humanitarian demining must be simple, robust and cheap. No one detector is optimal in all environments: variations in soil conductivity, and more importantly, frequency dependent soil magnetic susceptibility can favor one design over another. In particular, soils containing magnetic minerals can have as a result, a frequency dependent magnetic susceptibility which overlaps or coincides with the frequency range used for mine detection. Such soils are common enough that appropriate technology to understand and deal with these effects can make the dangerous job of humanitarian demining somewhat safer.

The Geophysics Lab of the University of Toronto is attempting to improve the technology in two ways. (supported by the Canadian Centre for Mine Action Technologies (CCMAT)) is aimed at investigating how EMI field instruments for humanitarian demining might be improved. The first is by constructing a better laboratory instrument to make measurements of the electromagnetic properties of difficult soils, in particular of frequency dependent magnetic susceptibility, and by finding semi-analytic representations of these responses suitable for modeling purposes. Based on experiments with a prototype, two production versions of this EMI spectrometer instrument are being built, with noise levels of the order of a few times 10^{-5} S.I. units, over a frequency range of 100 Hz to about 70 kHz. The second approach is by coding the software to allow such data to be used effectively in the simulation of detector performance. This involves assembling a number of induction algorithms into a single simulation code with a straightforward GUI, intended to be public domain as a MATLAB code. The final version of the code, when completed, is to handle single or multiple transmitter and receiver coils of circular or polygonal shape, general transmitter current waveforms, arbitrary transmitter orientations and survey paths, small targets with frequency-dependent anisotropic responses (permitting both magnetic and inductive responses to be calculated), embedded in multi-layered half spaces with both conductivity and frequency-dependent susceptibility (so-called "difficult soils").

Keywords: Electromagnetic induction, Humanitarian Demining, Frequency-dependent susceptibility

INTRODUCTION

With support from Defense Research and Development Canada's program on humanitarian demining, we are developing software tools to help simulate the performance of electromagnetic induction (EMI) metal detectors of arbitrary design. In order to make valid simulations, we need quantitative descriptions of the induction response of mine-like target objects and of the electromagnetic properties of the soils in which the mines may be hidden. The information must be valid in the spectral range employed in typical mine detectors, 1 to 100 kHz, and should preferably cover from 0.1 kHz to 1 MHz. Unfortunately, with the exception of a few

susceptibility amplitude measurement at two frequencies (465 and 4650 Hz) using the Bartlington susceptibility meter (ref), few spectral data are available in the scientific literature.

Modern anti-personnel mines typically contain only a few grams or less of electrically conductive metal; often only ~ 1 mm to ~ 1 cm in extent. Thus, it has become necessary to increase the basic sensitivity of mine detectors to a level where discrimination between the desired EMI response from a significant target object and the unwanted responses from magnetic minerals naturally present in the soil is often the key issue --- not just simple target detectability. Furthermore, in wet locales such as marine beaches, the bulk electrical conductivity of the environment may possibly generate significant

interference. Therefore, most modern detectors are designed to be unresponsive to ideally permeable, non conductive materials and they use a spectral window below about ~100 kHz to minimize possible response from the bulk conductivity of the soil.



Figure 1. EMI detector for humanitarian demining use.

Although experience with the best modern EMI metal detectors has been relatively favourable, it has also revealed that many naturally magnetic soils do not behave as ideally permeable materials. Some may exhibit a frequency dependent, complex, magnetic susceptibility capable of confusing most detectors (sometimes termed *viscous magnetization* or VM, (Dunlop, D.J. and O. Ozdemir, 1997)). In the few cases where the effect has been investigated seriously, it usually is attributed to the presence of very fine grained ferromagnetic material close to the Néel superparamagnetic transition (Mullins and Tite, 1973). The problem was first noticed in Australia where EMI metal detectors are widely used in prospecting for gold nuggets in weathered soil, and at least one manufacturer there (MineLab) offers an instrument that can be trained to reject a VM background signal (Candy, 1996).

It is, of course, possible to estimate by theoretical methods (e.g. Das, 2005) the EMI response characteristics of conductive and permeable objects like those present in mines. However, the metal objects in actual mines may have poorly known compositions and odd shapes, so direct experimental confirmations seem necessary. Likewise, the volume magnetic susceptibility of typical soils (real or complex) can be estimated from the limited available studies, and electrical conductivity can be estimated from porosity and water salinity data. However, because reality often differs from prior expectations, we believe that direct observation would be better.

THE EMI SPECTROMETER

The spectrometer (West and Bailey, 2005) uses a pair of transmitter coils in a Helmholtz configuration and a pair of receiver coils also in a Helmholtz configuration, to achieve uniform sensitivity over as large a volume as possible. Samples of standard paleomagnetic size (12.9 ml) are easily accommodated, and even over twice this sample volume, the sensitivity does not vary by more than about 5%. An additional pair of reference coils is used to null the directly coupled signal. A small number of turns in the coils keeps self-resonances above about 0.5 MHz. The signal is locally preamplified before sending to a PC computer for processing.

Signal acquisition is done with a high-end commercial sound card in a PC, driven by MATLAB. A wide-band signal generated with this card is used to drive the transmitter. current input to the transmitter coils is used. The received signal is sampled at 192 kHz; a frequency-dependent susceptibility is computed by correlation and spectral division. A null (sample-free) measurement run is incorporated to reduce the effects of instrument drift. Measurement of a sample can take as little as 30 seconds, including loading and unloading. Tensor measurements for anisotropic samples are also possible, utilizing a rotating sample holder and a more complex measurement protocol.

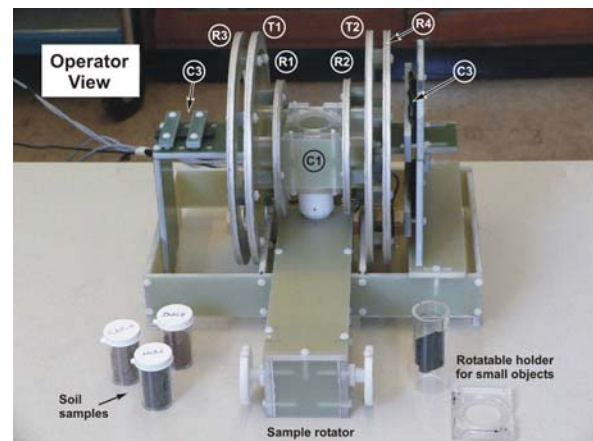


Figure 2. Prototype of wideband EMI spectrometer. The prototype does not have a case. Not shown are the preamplifier, the transmitter unit or the computer used for signal acquisition.

Magnetic soils that present a serious problem for mine detection usually have susceptibilities of 1 mSIU or greater. Thus the sensitivity objective for the instrument was an ability to delineate accurately the susceptibility spectrum of a standard 12.9 ml specimen with a susceptibility of about 1 mSIU. Therefore, base level drifts and noise should not much exceed 0.01 mSIU over the measurement bandwidth of 100 Hz to about 70 kHz.

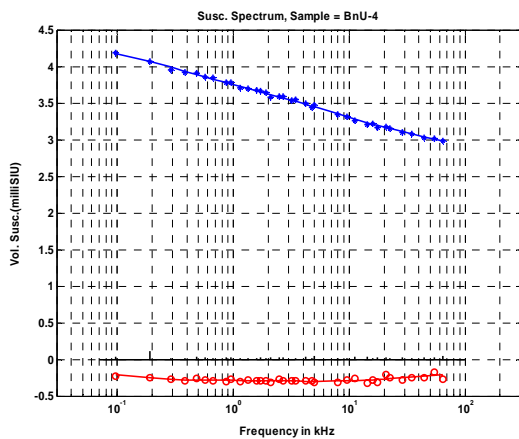


Figure 3. Wide-band susceptibility response of a “problem soil” from Bosnia, in milliSI units. In-phase as blue crosses; quadrature response (emulating an induction response) of about $-3 \cdot 10^{-4}$ SI as red circles.

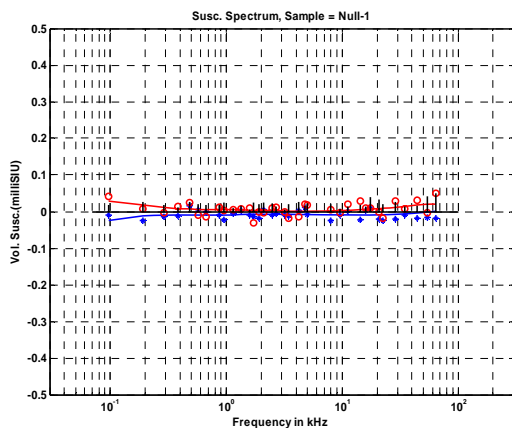


Figure 4. Wideband noise floor of the instrument a measurement, from an empty sample holder, close to 10^{-5} SI units. Colors and symbols as in Figure 3.

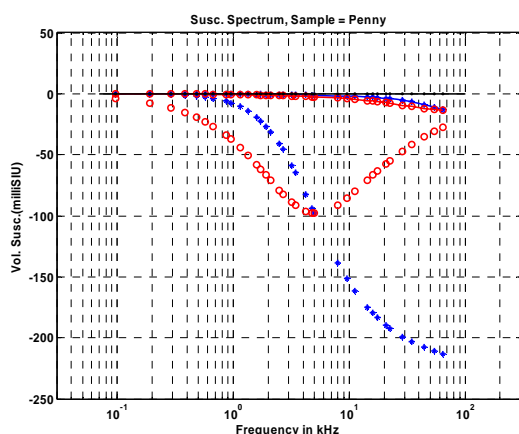


Figure 5. Induction response of a small metal object (Canadian penny) in two orthogonal directions, expressed as a equivalent susceptibility of a sample volume of 12.9 ml. Colors and symbols as in Figure 3.

SIMULATION CODE

The main challenge in preparing the simulation code is not the computation of electromagnetic responses of soils and targets. In general, targets are small, so point target responses are appropriate (that is, the inducing field can be assumed uniform over the region of the target, and the fields of the target at the receiver can be assumed to be those of a point dipole). With targets typically buried less than 10 cm, shielding by overlying soil is typically small and often negligible. Standard algorithms for calculating fields in a layered environment have been available in the literature for some time (e.g. Grant and West, 1965; Wait, 1982; Ward, S and Hohmann, 1987; Guptasarma and Singh, 1997). The primary goal in coding was to achieve usability by instrument designers on a wide range of instrument designs, with arbitrary coil arrangements, transmitter waveforms, and signal acquisition and processing, as well as the ability to use target and soil response data based on both theoretical models and experimental data such as produced by the spectrometer above.

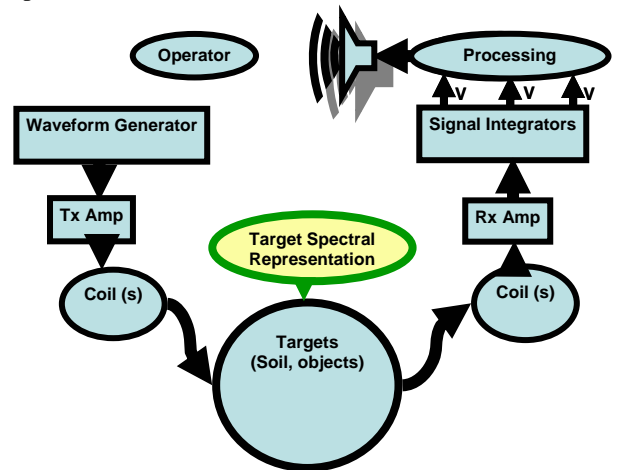


Figure 6. Components of the detection simulation model used by the code.

Accordingly, effort has been directed towards an effective GUI and flexible methods of describing instrument configuration and target characteristics (Bailey and West, 2006). Target responses are characterized in terms of a pole-zero description (West and Bailey, 2006) in the complex frequency plane, a separate response for each principal axis of the target if required.. The exponential decays associated with each pole can be pre-processed with the instrument signal processing algorithms. This permits a simple sum over these decay modes to be performed at each instrument location in a simulated survey, in which only the instrument-target coupling amplitudes need be recomputed at each location, not the full frequency or waveform dependence.

The final suite of models which the code is planned to handle are summarized in Table 1. The code is written in MATLAB. This facilitated several important features: users can enter theoretical responses as MATLAB formulae, which the code will understand; all of MATLAB's edittable plotting facilities are available, and the GUI permits exporting numerical results to the MATLAB workspace, where users can do any further analysis of them with their own code.

	HCC	HPC	TPD	TPC
FS	U,S	U	U,S	U
LHS	U,S		U,S	
FD3DS	U	U	U	

Table 1. Design goals of the code. Sensor abbreviations are HCC - horizontal circular coils; HPC - horizontal polygonal coils; TPD - tilted point dipoles; TPC - tilted polygonal coils. Target and host abbreviations are: UFDPT - unshielded frequency-dependent point target; SFDPT - shielded frequency-dependent point target; FS - free space; LHS - conductive layered half-space with conductivity and frequency-dependent susceptibility specified in each layer; FD3DS - 1, 2, or 3D weak susceptibility distribution with global frequency-dependence.

CONCLUSIONS

We have developed an instrument for wideband measurements of magnetic susceptibility over the frequency range 100 Hz to 70 kHz. We have developed code for utilizing this data in the calculation of the induction response of small metal targets embedded in soils with frequency dependent magnetic permeability. These two tools should be useful in producing better designs for field instruments for humanitarian demining, which can distinguish between the quadrature response of the desired metal targets and the quadrature response caused by the frequency-dependent magnetic susceptibility of problem soils.

ACKNOWLEDGEMENTS

This work was supported by the Canadian Centre for Mine Action Technologies (CCMAT) of Defense Research and Development Canada (DRDC) as part of contract No. W7702-03R942/001/EDM. We gratefully acknowledge the assistance and guidance provided by DRDC personnel in at Suffield, Alberta, and especially the help from Dr. Yoga Das, technical authority for the contract. We also acknowledge the assistance provided by Dr Rob Moucha.

REFERENCES

- Bailey, R.C. and West, G.F., 2006, Characterizing mine detector performance over difficult soils, in Proc. SPIE 6217, Detection and Remediation Technologies for Mines and Minelike Targets XI, J.T. Broach, R.S. Harmon, and J. Holloway, eds., 62170P_1-621702_10.
- Candy, B. H., "Pulse Induction Time Domain Metal Detector", United States Patent Number 5 576 624, November 1996.
- Das, Y. 2005, Electromagnetic induction response of a target buried in conductive and magnetic soil, in Proc. SPIE 5794, Detection and Remediation Technologies for Mines and Minelike Targets X, R.S. Harmon, J.T. Broach, and J. Holloway, eds., 263--274,.
- Dunlop, D.J. and O. Ozdemir, 1997, Rock Magnetism, Cambridge University Press.
- Grant, F.S. and West, G.F., 1966, Interpretation theory in applied geophysics, McGraw-Hill, New York.
- Guptasarma, D. and Singh, B., 1997, New digital linear filters for hankel j_0 and j_1 transforms, Geophysical Prospecting 45, 745--762.
- Mullins, C.E. and M.S. Tite, 1973, Magnetic viscosity, quadrature susceptibility, and frequency dependence of susceptibility in single-domain assemblies of magnetite and maghemite, Journal of Geophysical Research 78, 804--809.
- Wait, J.R., 1982 Geo-electromagnetism, Academic Press.
- Ward, S.H. and Hohmann, G., 1987, Electromagnetic Methods in Applied Geophysics vol. 1, ch. Electromagnetic Theory for Geophysical Applications, Society of Exploration Geophysicists.
- West, G.F. and Bailey., R.C., 2005, An instrument for measuring complex magnetic susceptibility of soils, in Proc. SPIE 5794, Detection and Remediation Technologies for Mines and Minelike Targets X, R.S. Harmon, J.T. Broach, and J. Holloway, eds., 124-135.
- West, G.F. and Bailey, R.C., 2006, Spectral representation, a core aspect of modelling the response characteristics of time-domain emi mine detectors, in Proc. SPIE 6217, Detection and Remediation Technologies for Mines and Minelike Targets XI, J.T. Broach, R.S. Harmon, and J. Holloway, eds., pp. 621702_1-621702_12